Is Indenyl a Stronger or Weaker Electron Donor Ligand than Cyclopentadienyl? Opposing Effects of Indenyl Electron Density and Ring Slipping on Electrochemical Potentials

Khiem T. Nguyen, Emily E. Lane, Colin D. McMillen, Jared A. Pienkos, and Paul S. Wagenknecht*
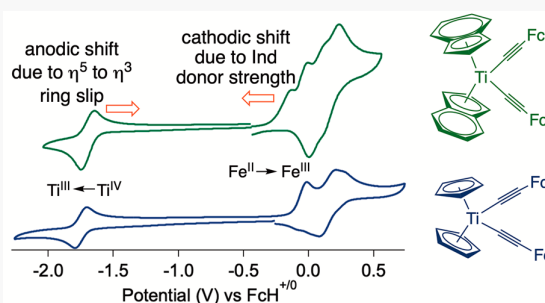
Read Online

ACCESS | Metrics & More | Article Recommendations | Supporting Information

ABSTRACT: Complexes of the type $^{R}Cp_2Ti(C_2Fc)_2$ (where ^{R}Cp = cyclopentadienyl or a substituted cyclopentadienyl) have high molar absorptivity Fe^{II} to Ti^{IV} metal-to-metal charge transfer (MMCT) absorptions and have been investigated for possible use as photoredox catalysts. Relative to $Cp_2Ti(C_2Fc)_2$, the MMCT shifts to higher or lower energy when ^{R}Cp is either a stronger or weaker donor ligand than Cp, respectively. The indenyl ligand (Ind) has been described in the literature as both a stronger and weaker donor ligand than Cp. Herein, we report the preparation of $Ind_2Ti(C_2Fc)_2$ and the complex with CuBr bound between the two alkynes, $Ind_2Ti(C_2Fc)_2CuBr$, in order to determine the effect that replacing Cp with Ind has on the MMCT absorption energy. The complexes are characterized by NMR and UV−

vis spectroscopy, cyclic voltammetry, and X-ray crystallography in the case of $Ind_2Ti(C_2Fc)_2CuBr$. Relative to $Cp_2Ti(C_2Fc)_2$, the $Fe^{III/II}$ potential of $Ind_2Ti(C_2Fc)_2$ shifts cathodically and the $Ti^{IV/III}$ potential shifts anodically, resulting in a lower energy MMCT absorption. The $Ti^{IV/III}$ reduction wave is also chemically irreversible, with i_{pa}/i_{pc} approaching unity as the scan rate is increased from 10 to 500 mV/s. Examination of the literature reviewed in this report demonstrates that, in all cases, replacement of Cp with Ind leads to a cathodic shift of the potential for metal oxidation. However, replacement of Cp with Ind typically leads to an anodic shift of the reduction potential, leading some to suggest that Ind is a poorer e^- donor than Cp. In the context of the literature, these results are interpreted as indicating that Ind is a better electron donor than Cp, but that reduction induces an η^5 to η^3 haptotropic shift that is rapid on the electrochemical time scale, stabilizing the reduction product, resulting in an anodic shift of the $Ti^{IV/III}$ reduction. Furthermore, these opposing effects are not unique to this system.

INTRODUCTION

Since the initial discovery of ferrocene nearly 70 years ago,[1,2] organometallic complexes with cyclopentadienyl (Cp) ligands have been among the most extensively investigated and applied molecules in the realm of organometallic structure and reactivity. Though less investigated, indenyl (Ind) complexes often show improved catalytic activity relative to their cyclopentadienyl complex analogues.[3] The improved catalytic behavior is often related to the increased rate of substitution chemistry for indenyl metal complexes. This "indenyl effect" was first reported in 1969 for a migratory insertion reaction where $(Ind)Mo(CO)_3CH_3$ reacts with PPh_3 to give $(Ind)Mo(CO)_2PPh_3COCH_3$.[4] The rate acceleration with respect to the Cp complex was suggested to be the result of a more favorable η^5 to η^3 ring slip for the indenyl complexes compared to the cyclopentadienyl complexes (Figure 1). Such a ring slip decreases the electron count at the central metal, thus lowering the energy barrier for coordination of the additional ligand necessary to induce the migratory insertion.[4,5] Since that initial discovery, the indenyl effect has been shown to be a quite general phenomenon for indenyl complexes.[5−7] The gener-
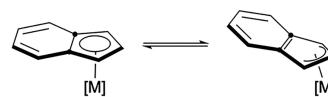

Figure 1. η^5 to η^3 haptotropic shift.

ation of aromaticity in the fused benzo ring has typically been cited for the increased ability of indenyl to undergo η^5 to η^3 ring slip,[4−6] but more recent computational studies suggest that the indenyl effect is related to the relative metal π-ligand bond strengths for Cp and Ind in each binding mode.[7]

This differential behavior of the Cp and Ind complexes has stimulated investigations into the relative electronic nature of these two ligands. Several investigations suggest that the Ind ligand is more electron-rich than the Cp ligand, whereas others

suggest Ind is more electron-poor. For example, photoelectron spectroscopy on d^6 and d^8 complexes has suggested that for such complexes, the Ind ligand is more electron-rich than the Cp ligand.[8,9] This is consistent with what is observed in infrared spectroscopic investigations[10] and redox potentials for metal oxidation in d^6 complexes.[6,11] This contrasts with what reduction potentials of η^5-Ind complexes suggest, where replacement of Cp with Ind typically results in an anodic shift of the metal-centered reduction,[12−14] leading some authors to suggest that Ind is a poorer donor compared to Cp.[14]

Recently, we have been interested in complexes of the type $^RCp_2Ti(C_2Fc)_2$ (Figure 2) which show an intense electronic

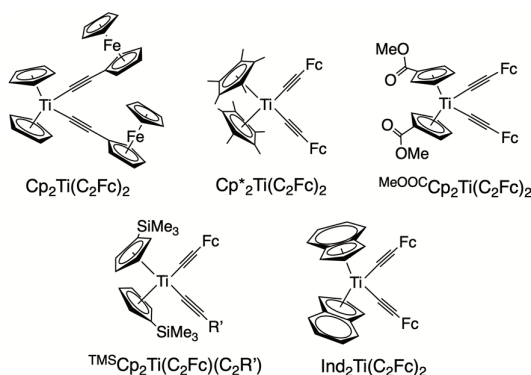**Figure 2.** $Fe^{II}-Ti^{IV}$ complexes discussed in this paper along with abbreviations used. $^RCp_2Ti(C_2Fc)_2$ is the general abbreviation used to refer to the complexes with two ethynylferrocene ligands and any substitution on the Cp ring (top row).

Fe^{II} to Ti^{IV} metal-to-metal charge-transfer (MMCT) absorption.[15−17] The excited state $^RCp_2Ti(C_2Fc)_2^{+/0}$ potential is estimated to be more negative than -1.30 V vs $FcH^{+/0}$, suggesting that these complexes may be potent excited state reducing agents.[15] Moreover, the energy of the CT band can be tuned by the nature of the substituents on the Cp ligands. For example, when ^RCp is pentamethylcyclopentadienyl (Cp*), there is a cathodic shift of the $Ti^{IV/III}$ reduction potential relative to that of the corresponding Cp complex and a concomitant blue-shift of the Fe^{II} to Ti^{IV} MMCT.[15] On the other hand, when ^RCp is a methyl ester substituted cyclopentadienyl ($^{MeOOC}Cp$), the $Ti^{IV/III}$ reduction potential shifts anodically relative to the Cp complex, resulting in a red-shift of the Fe^{II} to Ti^{IV} MMCT (Figure 3).[17] Given the inconsistent statements in the literature regarding the donor properties of Ind vs Cp, we set out to investigate the corresponding $Ind_2Ti(C_2Fc)_2$ complex (Figure 2), partly out of curiosity regarding whether the Fe^{II} to Ti^{IV} MMCT would red-shift or blue-shift relative to its Cp analogue.

Herein, we report the synthesis and characterization of $Ind_2Ti(C_2Fc)_2$, and a derivative where CuBr is bound between the alkynes. We focus on seemingly incompatible findings regarding the electrochemistry of $Ind_2Ti(C_2Fc)_2$. Chiefly, the $Fc^{+/0}$ potential for the bound ethynylferrocene ligand shifts cathodically relative to the corresponding Cp complex, consistent with Ind being more electron-rich and there being an inductive effect through to the Fc. However, there is a corresponding slight *anodic* shift of the $Ti^{IV/III}$ reduction potential, consistent with what is typically observed for metal-centered reductions upon replacement of Cp with Ind, but
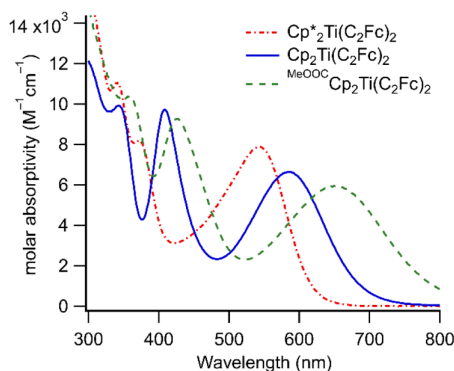

Figure 3. UV−vis absorption spectra in CH_2Cl_2 for the $^RCp_2Ti-(C_2Fc)_2$ complexes. The color of the curves approximates the color of each complex.

inconsistent with Ind being more electron-rich than Cp. The observation that Ind shifts the oxidation of Fe^{II} in the cathodic direction and the reduction of Ti^{IV} in the anodic direction, all within the same molecule, suggests that this might be a general phenomenon, rather than the direction of the shift being dependent on the electronic properties of the metal on which the Cp/Ind substitution is implemented. This phenomenon is explored along with the impact of these electrochemical potentials on the energy of the MMCT transition in this complex.

RESULTS

Synthesis and General Characterization. The complexes investigated herein were prepared according to the literature procedures for the analogous complexes with Cp ligands (Figure 4).[15,16] The syntheses were performed under
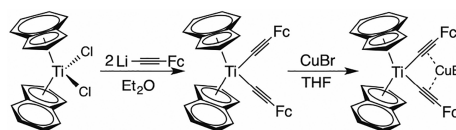

Figure 4. General synthetic scheme for the complexes reported herein.

Ar in anhydrous conditions, but the products are stable to atmospheric conditions and are also photostable. Thus, all purifications and subsequent manipulations were performed on the benchtop without the need for inert atmosphere or anhydrous solvent. Like the corresponding Cp complexes, the Ind complexes are sensitive to acid hydrolysis. Thus, $CDCl_3$ for NMR spectroscopy is passed through activated alumina to remove any acidic impurities. In $CDCl_3$, the indenyl hydrogens of $Ind_2Ti(C_2Fc)_2$ are overlapping, but these are well resolved in C_6D_6 (Supporting Information, Figure S1). The ferrocenyl hydrogens appear as a singlet at 4.20 ppm for the unsubstituted Cp ring and two apparent triplets (dd, $J_1 = J_2$) at 4.00 and 4.40 ppm for the substituted Cp ring. The indenyl hydrogens on the C_5 ring appear as a doublet at 6.17 ppm and a triplet at 6.20 ppm, and those on the C_6 ring as two doublets of doublets at 7.00 and 7.51 ppm.

Coordination of CuBr occurs between the alkynyl ligands as has been previously reported for bis-alkynyl titanocenes.[16,18−20] Diagnostic of this coordination is a shift of

$\nu_{C\equiv C}$ from 2048 cm^{-1} for the parent Ind$_2$Ti(C$_2$Fc)$_2$ to 1986 cm^{-1} for Ind$_2$Ti(C$_2$Fc)$_2$CuBr, in agreement with previous examples where Cu^I was coordinated between the alkynes.[16,18−20] This structure was confirmed using X-ray crystallography (Figure 5, and Supporting Information Table
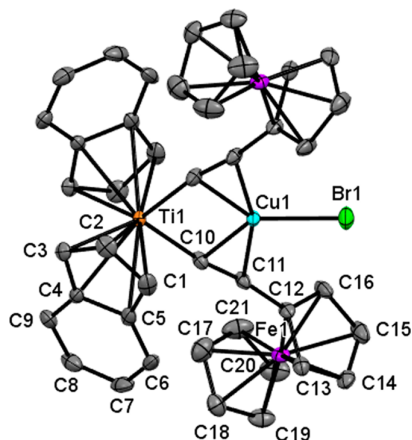

Figure 5. Structure of Ind$_2$Ti(C$_2$Fc)$_2$CuBr shown as 50% probability ellipsoids. Hydrogen atoms omitted for clarity. Key interatomic distances: Cu(1)−C(10) 2.048(4) Å; Cu(1)−C(11) 2.232(4) Å; Cu(1)−Ti(1) 2.8064(11) Å; Cu(1)−Br(1) 2.2818(8) Å; C(10)−C(11) 1.231(6) Å; Ti(1)−C(10) 2.075(4) Å; Ti(1)−C(1) 2.397(4) Å; Ti(1)−C(2) 2.344(4) Å; Ti(1)−C(3) 2.344(4) Å; Ti(1)−C(4) 2.443(3) Å; Ti(1)−C(5) 2.505(4) Å. Key interatomic angles: C(10)−Ti−C(10a) 93.4(2)°; Ti(1)−C(10)−C(11) 167.3(3)°; Cp$_{centroid}$−Ti(1)−Cp$_{centroid}$ 135.8°.

S1 and Figures S3, S4). The structure clearly shows nearly ideal η^5 coordination of the Ind ligands to Ti as indicated by two key distortion parameters: the slip fold parameter, Δ, which is the difference in average M−C bond distances to the ring junction carbons, C(4) and C(5), vs the adjacent carbons C(1) and C(3); and the hinge angle, HA, defined as the angle between the planes defined by [C(1), C(2), C(3)] and [C(1), C(3), C(4), C(5)]. Indenyl complexes are considered to exhibit η^5 coordination if Δ and HA are less than 0.25 Å and 10°, respectively.[6,21,22] For Ind$_2$Ti(C$_2$Fc)$_2$CuBr, Δ = 0.10 Å, and HA = 3.1°. The additional steric bulk of the fused benzo ring has only a small impact on the bond angle between the Ti and the two C$_5$ centroids. Chiefly, it has expanded from 134.5° in Cp$_2$Ti(C$_2$Fc)$_2$CuBr[16] to 135.8° in the analogous Ind complex. There exists a corresponding expansion of the C(10)−Ti−C(10a) bond angle from 91.13(10)° to 93.4(2)° and thus a shortening of the Ti−Cu distance from 2.8901(6) to 2.8064(11) Å. The molecule itself has twofold rotational symmetry. Packing of molecules (Supporting Information, Figure S4) occurs primarily through weak intermolecular C−H···π interactions between Fc and Ind ligands along the a-axis, as well as weak intermolecular C−H···Br interactions along the b-axis.

The UV−vis absorption spectra for both Ind$_2$Ti(C$_2$Fc)$_2$ and Ind$_2$Ti(C$_2$Fc)$_2$CuBr, in CH$_2$Cl$_2$ (Figure 6), show the presence of two absorptions in the visible region. By analogy with the Cp$_2$Ti(C$_2$Fc)$_2$ complexes,[15] the absorptions near 400 nm are assigned to an Ind to Ti LMCT and the absorptions near 600 nm assigned to an Fe^{II} to Ti^{IV} MMCT. As with other complexes in this series, the coordination of CuBr results in a slight redshift and attenuation of the molar absorptivity.[16]
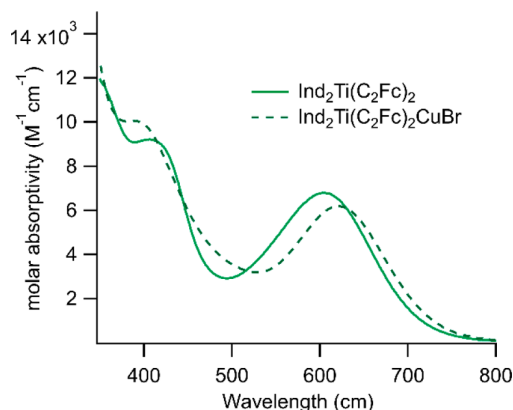

Figure 6. UV−vis absorption spectra in CH$_2$Cl$_2$ of Ind$_2$Ti(C$_2$Fc)$_2$ and Ind$_2$Ti(C$_2$Fc)$_2$CuBr.

Similar behavior is observed in THF (Supporting Information, Figure S5).

Electrochemistry. The voltammogram of Cp$_2$Ti(C$_2$Fc)$_2$ has been previously reported and shows a chemically reversible Ti$^{IV/III}$ reduction in the cathodic scan.[15] The anodic scan reveals a chemically irreversible 2e$^-$ Fe$^{III/II}$ couple followed by a chemically reversible 2e$^-$ couple (Figure 7, bottom). The
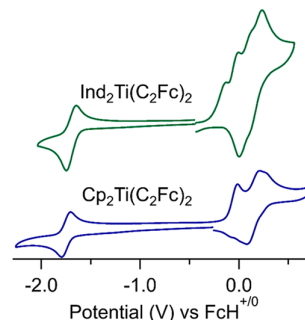

Figure 7. Cyclic voltammogram of Ind$_2$Ti(C$_2$Fc)$_2$ (top) and Cp$_2$Ti(C$_2$Fc)$_2$ (bottom), ~1 mM in CH$_2$Cl$_2$ (0.1 M n-Bu$_4$NClO$_4$), glassy carbon working electrode, Ag$^{+/0}$ reference electrode, Pt auxiliary electrode, scan rate = 100 mV/s, N$_2$ purged. Cyclic voltammograms of FcH are recorded before and after the cyclic voltammogram and the potentials are corrected for the potential of FcH$^{+/0}$ vs Ag$^{+/0}$. Due to the irreversibility in both the cathodic and anodic scans of Ind$_2$Ti(C$_2$Fc)$_2$, each direction for that complex is recorded separately.

irreversible nature of this first oxidation has been attributed to subsequent rapid heterolytic Ti−C bond cleavage.[15,23,24] During this cleavage, 1e$^-$ from each Ti−C bond serves to reduce Fc$^+$ back to Fc, while the remaining e$^-$ is involved in the formation of a new C−C bond to generate FcC$_4$Fc (eq 1). The reversible oxidation of FcC$_4$Fc appears slightly anodic of the first irreversible oxidation and consists of two closely spaced 1e$^-$ Fe$^{II/III}$ oxidations.

$$\text{Cp}_2\text{Ti}\Big\langle^{\text{C}_2\text{Fc}}_{\text{C}_2\text{Fc}} \xrightarrow{-2e^-} \text{Cp}_2\text{Ti}\Big\langle^{\text{C}_2\text{Fc}^+}_{\text{C}_2\text{Fc}^+} \longrightarrow [\text{Cp}_2\text{Ti}^{IV}]^{2+} + \text{FcC}_4\text{Fc} \quad (1)$$

The cyclic voltammogram of Ind$_2$Ti(C$_2$Fc)$_2$ shows some notable differences (Figure 7, top). First, the Ti$^{IV/III}$ reduction is no longer chemically reversible, with i_{pa}/i_{pc} < 1. A scan rate dependence (Supporting Information, Figure S6) shows that

i_{pa}/i_{pc} approaches unity with increased scan rate (10 mV/s to 500 mV/s), suggesting an EC mechanism. Second, rather than a single irreversible 2e⁻ Fe$^{III/II}$ wave in the anodic scan prior to the FcC$_4$Fc oxidation, two waves are observed with similar currents to the 1e⁻ Ti$^{IV/III}$ reduction. Thus, these are ascribed to 1e⁻ oxidations. An anodic scan of Ind$_2$TiCl$_2$ shows no features in this potential range, suggesting that these waves must both be due to the oxidation of Fc. Reversing the scan after each of these oxidations demonstrates that each is chemically irreversible (Supporting Information, Figure S7). The reversible wave at anodic potentials to these two irreversible waves resembles that of FcC$_4$Fc. Indeed, spiking the solution with a sample of FcC$_4$Fc supports the assignment of FcC$_4$Fc as the product of the irreversible oxidations. Third, for the Ind complex relative to the Cp complex, there is an anodic shift of the Ti$^{IV/III}$ potential but a cathodic shift of the Fe$^{III/II}$ potential (Figure 7 and *vide infra*).

As has been observed previously for ^{R}Cp$_2$Ti(C$_2$Fc)$_2$ complexes,[16] coordination of CuBr to Ind$_2$Ti(C$_2$Fc)$_2$ stabilizes the complex toward oxidation, resulting in the observation of two separate, chemically reversible, 1e⁻ oxidations in the cyclic voltammograms (Figure 8, Table 1). The absence of an anodic
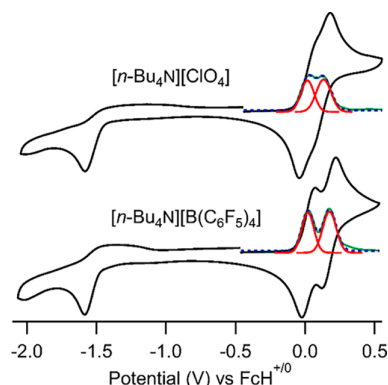

Figure 8. CVs and DPVs for Ind$_2$Ti(C$_2$Fc)$_2$CuBr with two different supporting electrolytes. Other than supporting electrolyte, conditions are the same as described in Figure 7. For the DPV insets, the green line is the experimental DPV, the red lines correspond to the individual Gaussian fits used to fit the data, and the dashed line represents the sum of the individual Gaussian fits.

Table 1. Fe$^{III/II}$ Potentials for Ind$_2$Ti(C$_2$Fc)$_2$CuBr and Cp$_2$Ti(C$_2$Fc)$_2$CuBr with Different Supporting Electrolytes

compound	electrolyte	$E_{1/2}(1)^{a,b}$	$E_{1/2}(2)^{a,b}$
Ind$_2$Ti(C$_2$Fc)$_2$CuBr	[n-Bu$_4$N][ClO$_4$]	0.018	0.134
Ind$_2$Ti(C$_2$Fc)$_2$CuBr	[n-Bu$_4$N][B(C$_6$F$_5$)$_4$]	0.021	0.176
Cp$_2$Ti(C$_2$Fc)$_2$CuBr	[n-Bu$_4$N][ClO$_4$]	0.024	0.137
Cp$_2$Ti(C$_2$Fc)$_2$CuBr^{c}	[n-Bu$_4$N][B(C$_6$F$_5$)$_4$]	0.016	0.160

^{a}All electrochemical $E_{1/2}$ values are from Gaussian fits of the DPV. ^{b}All potentials are reported vs FcH$^{+/0}$. ^{c}From ref 16.

feature in the analogous voltammogram for Cp$_2$Ti-(C$_2$Ph)$_2$CuBr[16] precludes ascribing either feature in Ind$_2$Ti-(C$_2$Fc)$_2$CuBr to a Cu$^{II/I}$ redox couple. Thus, these are ascribed to two separate Fe$^{III/II}$ couples, indicating some degree of electronic communication between the two redox-active sites. When the supporting electrolyte, [n-Bu$_4$N][ClO$_4$], is replaced with [n-Bu$_4$N][B(C$_6$F$_5$)$_4$], the redox splitting, as measured by the differential pulse voltammograms (DPV), increases from

116 mV to 155 mV. This increased redox splitting in the presence of a less coordinating supporting electrolyte is typically interpreted in terms of increased electrostatic (through-space) interactions that occur between the redox active termini when ion-paring between the supporting electrolyte and the oxidized species is decreased (i.e., ion pairing with B(C$_6$F$_5$)$_4$⁻ is weaker than with ClO$_4$⁻).[16,25,26]

■ DISCUSSION

The majority of features observed for Ind$_2$Ti(C$_2$Fc)$_2$ and Ind$_2$Ti(C$_2$Fc)$_2$CuBr have been observed for other complexes in the ^{R}Cp$_2$Ti(C$_2$Fc)$_2$ series.[15,16] These are briefly discussed, followed by a focus on the peculiar nature of the redox potentials of the first oxidation and reduction of the parent Ind$_2$Ti(C$_2$Fc)$_2$.

Like all of the complexes in this series, oxidation of Ind$_2$Ti(C$_2$Fc)$_2$ is followed by rapid decomposition on the electrochemical time scale to give the electrochemically active FcC$_4$Fc. The complex can be stabilized by binding of CuBr between the alkynes. The Ind$_2$Ti(C$_2$Fc)$_2$CuBr complex shows two separate and reversible 1e⁻ waves corresponding to the sequential oxidation of the two Fc termini. The redox splitting is in the same range as those observed for other complexes in the ^{R}Cp$_2$Ti(C$_2$Fc)$_2$CuBr series.[16] For those complexes, no evidence of electronic coupling in the form of an Fe^{II}/Fe^{III} intervalence charge-transfer (IVCT) band was observed. Thus, the possibilities of through-space interactions, inductive effects, and stepwise coupling through a redox-active bridge were hypothesized.[16] For that series, a correlation was observed between the magnitude of the redox-splitting and the electron-density on the titanocene. For example, the magnitude of the redox-splitting was greater for the more electron-rich titanocene, Cp*$_2$Ti(C$_2$Fc)$_2$CuBr, than for Cp$_2$Ti(C$_2$Fc)$_2$CuBr (163 mV vs 144 mV with [n-Bu$_4$N][B(C$_6$F$_5$)$_4$] as the supporting electrolyte).[16] Given that the redox splitting for Ind$_2$Ti(C$_2$Fc)$_2$CuBr is 155 mV under the same conditions, that would suggest that Ind lies between Cp* and Cp in terms of its electron donor properties, consistent with summaries of photoelectron spectroscopy and redox potentials for oxidation of η^5-indenyl complexes.[6]

One notable difference between the electrochemistry of Ind$_2$Ti(C$_2$Fc)$_2$ and others in the ^{R}Cp$_2$Ti(C$_2$Fc)$_2$ series is that rather than observing a single 2e⁻ wave for the simultaneous oxidation of the two Fc termini, two 1e⁻ waves are observed. The first of these two oxidations can be assumed to be the oxidation of one of the Fc ligands of intact Ind$_2$Ti(C$_2$Fc)$_2$. However, because this oxidation is irreversible, the species remaining at the electrode surface are no longer defined. Thus, the identity of the species being oxidized in the second irreversible oxidation wave is not known. It is likely that one or both ethynylferrocene ligands rapidly dissociate after the first oxidation. Thus, the second wave is presumably the oxidation of a dissociated ethynylferrocene or a bound ethynylferrocene after only one has dissociated. It is unclear why the Ind ligand results in this separation in potentials that is not observed for any of the other ^{R}Cp$_2$Ti(C$_2$Fc)$_2$ complexes. Previous reports have interpreted the 2e⁻ wave for these previously characterized ^{R}Cp$_2$Ti(C$_2$Fc)$_2$ complexes in terms of there being no electronic communication between the two Fc termini, and no intermediate decomposition step.[15,16,23,24]

Regardless of the nature of this difference in behavior, the potentials of the first oxidation step for each complex can be compared. For the Cp*,[15] Ind, and Cp[15] complexes, the Fe$^{III/II}$

potentials are −0.22, −0.21, and −0.08 V, respectively. This is again consistent with Ind being a superior donor ligand to Cp and a slightly weaker donor than Cp*, and there being an inductive effect on the Fe$^{III/II}$ potential. Furthermore, this is consistent with literature reports where the oxidation of Ind metal complexes always occurs at more cathodic potentials than the corresponding Cp complexes (Table 2). Not surprisingly, the coordination of CuBr mitigates this inductive potential difference (Table 1) as has been observed for other complexes in this series.[15,16]

Table 2. Comparison of Electrochemical Potentials for Cp and Ind Complexes[a]

compound	ox	red	solvent	electrolyte	ref
CpRuCl(PPh$_3$)$_2$	0.56	-	CH$_2$Cl$_2$	TBAPF$_6$	11
IndRuCl(PPh$_3$)$_2$	0.45	-	CH$_2$Cl$_2$	TBAPF$_6$	11
Cp$_2$Fe	0.49	-	CH$_2$Cl$_2$	TBAClO$_4$	27
IndCpFe	0.35	-	CH$_2$Cl$_2$	TBAClO$_4$	27
Ind$_2$Fe	0.21	-	CH$_2$Cl$_2$	TBAClO$_4$	27
Cp$_2$Ru	0.99	-	CH$_2$Cl$_2$	TBATFPB^b	28
IndCpRu	0.77	-	CH$_2$Cl$_2$	TBAPF$_6$	29
Ind$_2$Ru	0.55	-	CH$_2$Cl$_2$	TBAPF$_6$	29
Cp$_2$Os	0.79	-	CH$_2$Cl$_2$	TBATFPB^b	28
Ind$_2$Os	0.43	-	CH$_2$Cl$_2$	TBAPF$_6$	29
[Cp$_2$Co][ClO$_4$]	-	−1.16	H$_2$O	NaClO$_4$	12
[Ind$_2$Co][ClO$_4$]^c	-	−0.6	H$_2$O	NaClO$_4$	12
[Cp$_2$Co][PF$_6$]	-	−0.94	CH$_3$CN	TBAPF$_6$	30
[Ind$_2$Co][CF$_3$CO$_2$]	-	−0.51	CH$_3$CN	TBAClO$_4$	31
[Cp$_2$V(CO)$_2$][PF$_6$]^d	-	−0.93	THF	TBAPF$_6$	14
[Ind$_2$V(CO)$_2$][PF$_6$]	-	−0.56	THF	TBAPF$_6$	14
Cp$_2$V^e	-	−2.72	THF	TBAPF$_6$	14
Ind$_2$V^{d,e}	-	−2.38	THF	TBAClO$_4$	14
Cp$_2$Ti(CH$_3$)$_2$^{c}	-	−2.0	THF	TBAPF$_6$	13
Ind$_2$Ti(CH$_3$)$_2$^{c,d}	-	−1.9	THF	TBAPF$_6$	13
IndTiCl$_3$^{f}	-	−0.82	CH$_2$Cl$_2$	TBAPF$_6$	32
CpTiCl$_3$^{f}	-	−0.82	CH$_2$Cl$_2$	TBAPF$_6$	32

^{a}Potentials vs SCE unless otherwise indicated. ^{b}TBATFPB = Tetrabutylammonium tetrakis[3,5-bis(trifluoromethyl)phenyl]borate. ^{c}Only reported to nearest 0.1 V. ^{d}Irreversible. ^{e}Potential vs silver wire pseudoreference electrode, FcH$^{+/0}$ at 0.50 V. ^{f}Potential vs FcH$^{+/0}$.

Perhaps the most perplexing result is that the Ti$^{IV/III}$ potential for Ind$_2$Ti(C$_2$Fc)$_2$ is shifted anodically relative to the analogous Cp complex, suggesting that Ind is a *poorer* e⁻ donor than Cp. Thus, within the same complex, substituting Cp with Ind has shifted the Ti$^{IV/III}$ potential anodically while the Fe$^{III/II}$ potential is shifted cathodically. For every complex in this series *except Ind$_2$Ti(C$_2$Fc)$_2$*, both potentials shift in the same direction relative to the parent complex, **Cp$_2$Ti(C$_2$Fc)$_2$** (Table 3). This includes not only complexes where R groups on the Cp ring of the titanocene have been used to tune the electron density, but also where one of the two C$_2$Fc ligands has been replaced by a more electron withdrawing, substituted alkyne ligand, C$_2$R′ (Figure 2). This has been interpreted as an inductive effect through the Ti, i.e., ligand induced changes in e⁻ density at Ti^{IV} induce the same effect (albeit to a lesser degree) through the ethynyl bridge to the Fc.

As counterintuitive as it seems for Ind to produce an anodic shift of the Ti-centered reduction relative to Cp, a search of the literature shows this to be a general phenomenon (Table 2). In all but one of the reports we found, there was an Ind induced anodic shift (0.1 to 0.5 V). Only CpTiCl$_3$ did not follow this

Table 3. Redox Potentials for Complexes Discussed Herein[a]

complex	$E_{1/2}$ (Ti$^{IV/III}$)	$E_{1/2}$ (Fe$^{III/II}$)
Cp*$_2$Ti(C$_2$Fc)$_2$	−2.28	−0.22^b
Cp$_2$Ti(C$_2$Fc)$_2$	**−1.75**	**−0.08^b**
^{TMS}Cp$_2$(C$_2$Fc)(C$_2$PhCF$_3$)	−1.67	0.00^b
^{TMS}Cp$_2$(C$_2$Fc)(C$_2$CF$_3$)	−1.54	0.05
^{MeOOC}Cp$_2$(C$_2$Fc)$_2$	−1.46	−0.03^b
Ind$_2$Ti(C$_2$Fc)$_2$	−1.70^c	−0.21^{b,d}

^{a}Conditions given in Figure 7. ^{b}Irreversible wave. $E_{1/2}$ estimated as the half-wave potential. ^{c}Partially reversible wave. ^{d}Potential for the first oxidation.

pattern, exhibiting no Ti$^{IV/III}$ potential shift upon replacement of Cp with Ind.[32] Thus, the literature is consistent with what we have observed with respect to both a cathodic shift of the oxidation and an anodic shift of the reduction upon replacement of Cp with Ind. This suggests that the situation is more complex than a simple dependence on an inductive effect.

To unify these seemingly contradictory sets of experimental results, we suggest that the indenyl ligand is indeed more electron-rich (donating) than the Cp ligand, but that 1e⁻ reduction in indenyl complexes is accompanied by an η^5 to η^3 ring-slip, stabilizing the reduced form (due to a lowering of the donor number of the ligand from 6e⁻ to 4e⁻) and resulting in an anodic shift. This obviously requires that 1e⁻ reduction can indeed induce a ring-slip, and also that this ring-slip is rapid on the electrochemical time-scale. There is literature to support both of these factors. The first report of a redox induced η^5 to η^3 haptotropic shift involved the stepwise reduction of (η^5-Ind)$_2$V(CO)$_2$$^+$,[14] for which the intermediate 1e⁻ reduction product has been structurally characterized as (η^3-Ind)(η^5-Ind)V(CO)$_2$.[33] Furthermore, cyclic voltammetry suggests that the η^5 to η^3 ring slip equilibrium occurs rapidly on the electrochemical time scale.[14] Since that first example, several more examples of reductively induced haptotropic shifts of the indenyl ligand have been reported.[34,35] One particularly interesting example involves the stepwise reduction of (η^5-Ind)Mn(CO)$_3$ to its dianion.[35] The relatively small difference between the first and second reduction potentials (0.25 V) was taken as evidence that the 1e⁻ reduction intermediate is (η^5-Ind)Mn(CO)$_3$$^-$, and the 2e⁻ reduction product is (η^3-Ind)Mn(CO)$_3$$^{2-}$, having undergone a haptotropic shift that markedly stabilizes the dianionic reaction product. Thus, there is also a literature precedent for an η^5 to η^3 haptotropic shift of the indenyl ligand impacting the redox potential through stabilization of the reduction product.

Given the implication that Ind is more electron-rich than Cp, the effect of the haptotropic shift on the reduction potential must be larger than the effect of the differing donor capacity of Ind vs Cp. Furthermore, one might expect the η^5/η^3 equilibrium of the reduced species to shift further toward η^3 as the electron count of the metal increases. Indeed, for the aforementioned case where the 1e⁻ reduction product of (η^5-Ind)$_2$V(CO)$_2$$^+$ was structurally characterized as (η^3-Ind)(η^5-Ind)V(CO)$_2$, the reactant is an 18 e⁻ species and reduction without a haptotropic shift would result in a hypervalent 19 e⁻ species. Moreover, the largest anodic shifts of reductions in Table 2 occur for 18 e⁻ species. The one case where the reduction potentials for the Ind and Cp complexes are identical (i.e., IndTiCl$_3$ and CpTiCl$_3$) involves 12 e⁻ species, the lowest e⁻ count in Table 2. However, in the absence of any

haptotropic shift, one would have expected the reduction of the Ind complex to at least be slightly cathodic of the Cp complex due to differences in the donor strength. The fact that the redox potentials are the same indicates at least some equilibrium with the reduced η^5 species. Not surprisingly, the 16 e$^-$ Ind$_2$Ti(C$_2$Fc)$_2$ complex investigated herein shows a relatively modest (50 mV) anodic shift of the Ti$^{IV/III}$ reduction relative to its Cp analogue. One additional hint of a haptotropic shift accompanying the reduction of Ind$_2$Ti-(C$_2$Fc)$_2$ is the slight irreversibility of the Ti$^{IV/III}$ reduction wave, whereas this reduction is chemically reversible for all other complexes in the ^{R}Cp$_2$Ti(C$_2$Fc)$_2$ series.[15,17,23] Such irreversibility may be due to increased vulnerability to substitution upon an η^5 to η^3 ring slip, which could lead to decomposition.

The energy of the MMCT transition is worthy of discussion within the context of the ground and excited state potential-energy wells (Figure 9) showing the relationship between the
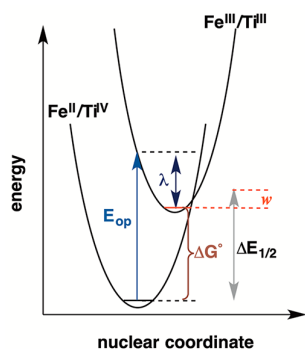

Figure 9. Potential well diagram showing relationship between observed electrochemical and optical parameters. Modified from ref 15.

energies of the vertical optical transition, E_{op}, the thermal transition, ΔG°, and the reorganization energy, λ, which can be estimated from the full-width at half-maximum, $\Delta \nu_{1/2}$, of the MMCT band (eq 2).[15,36] Figure 9 shows that subtraction of λ from E_{op} gives ΔG°.

$$\lambda = (\Delta \nu_{1/2})^2/2310 \text{ cm}^{-1} \qquad (2)$$

These values for ΔG° are compared with $\Delta E_{1/2}$, the potential difference between the Fe$^{III/II}$ couple and the Ti$^{IV/III}$ couple (Table 4). Given the smaller value of $\Delta E_{1/2}$ for Ind$_2$Ti(C$_2$Fc)$_2$ vs the Cp analogue, it is not surprising that the Fe^{II} to Ti^{IV} MMCT absorption for the Ind complex is red-

shifted compared to the Cp complex (16 450 cm^{-1} vs 17 120 cm^{-1}).

It is also important to point out that, although $\Delta E_{1/2}$ reasonably approximates ΔG°, it fails to account for the modified electrostatic interactions in the excited state.[37,38] That is, $\Delta E_{1/2}$ is the energy difference between the ground state and a state where the electron and hole are on different molecules, whereas the optical excited state has the electron and hole on the same molecule. The attractive interaction between an electron and a hole suggests that $\Delta E_{1/2}$ should overestimate ΔG° and approach zero as the charge separation distance increases. For previously studied complexes in this series,[15] the difference between $\Delta E_{1/2}$ and ΔG°, a Coulombic energy correction work term, w (Figure 9), is in a very similar range to those calculated for ferrocene to acceptor charge transfer through an ethylene bridge,[37] always being positive (Table 4).[15] However, for Ind$_2$Ti(C$_2$Fc)$_2$, $\Delta E_{1/2}$ *underestimates* ΔG° by 70 mV, resulting in a *negative* value for w. A possible explanation for this anomalous behavior employs the hypothesis that the Ti$^{IV/III}$ reduction potential for Ind$_2$Ti-(C$_2$Fc)$_2$ is anodically shifted because of the η^5 to η^3 haptotropic shift. Thus, there are likely two excited state potential surfaces: one where both indenyls are in the η^5 configuration and one with one indenyl having undergone a haptotropic shift. The latter will be at a lower energy than the former and further shifted from the ground state equilibrium geometry. As a result, the excited state accessed through the optical transition may be on a different potential surface than the one whose energy is estimated by electrochemical potentials.

CONCLUSIONS

Two new complexes with Fe^{II} to Ti^{IV} MMCT transitions, Ind$_2$Ti(C$_2$Fc)$_2$ and Ind$_2$Ti(C$_2$Fc)$_2$CuBr, have been prepared and characterized. Though many of the features of these complexes are similar to those of other ^{R}Cp$_2$Ti(C$_2$Fc)$_2$ complexes, the electrochemistry hints at some unusual properties resulting from the Ind ligand. Chiefly, relative to the corresponding Cp complex, the Ti$^{IV/III}$ reduction potential shifts anodically, while the Fe$^{III/II}$ potential shifts cathodically. Though some caution should be exercised in interpretation due to the irreversible nature of the Fc centered oxidations, an investigation of the literature shows that this is a general phenomenon. Namely, oxidation processes shift cathodically upon replacement of Cp with Ind, and reduction processes shift anodically (Table 2). Though the preponderance of literature suggests that Ind is more electron-rich than Cp, some suggest Ind is a poorer donor based on a comparison of reduction potentials. To the best of our knowledge, the complexes discussed herein comprise the first example where the effects of replacing Cp with Ind on both an oxidation

Table 4. Comparison of Spectroscopic and Electrochemical Parameters in CH$_2$Cl$_2$

complex	E_{op} (cm^{-1})	λ (cm^{-1})	ΔG° (cm^{-1})	ΔG° (V)	$\Delta E_{1/2}$ (w)
Cp*$_2$Ti(C$_2$Fc)$_2$[a]	18380	2790	15600	1.93	2.06 (0.13)
Cp$_2$Ti(C$_2$Fc)$_2$[a]	17120	4030	13100	1.62	1.67 (0.05)
^{MeOOC}Cp$_2$Ti(C$_2$Fc)$_2$[b]	15410	4880	10500	1.30	1.46 (0.16)
^{TMS}Cp$_2$Ti(C$_2$Fc)(C$_2$PhCF$_3$)[a]	16860	5000	11900	1.48	1.67 (0.19)
^{TMS}Cp$_2$Ti(C$_2$Fc)(C$_2$CF$_3$)[a]	15870	5150	10800	1.34	1.59 (0.25)
Ind$_2$Ti(C$_2$Fc)$_2$	16450	3830	12620	1.56	1.49 (−0.07)

[a]Values from ref 15. [b]Values from ref 17.

process and reduction process within the same molecule have been compared. These results are in agreement with the literature and suggest that the opposing potential shifts might be a general phenomenon, rather than the direction of the shift being dependent on either the d-electron count or total electron count at the metal. We hypothesize that Ind is indeed more electron-rich than Cp, but that an η^5 to η^3 haptotropic shift accompanies reduction, thus stabilizing the product, resulting in an anodic shift of the reduction potential. Such a haptotropic shift is much less likely for the corresponding Cp complex. Furthermore, because most known indenyl complexes are η^5, no ring-slipping is expected upon oxidation since such a shift would further lower the electron count of the metal. This hypothesis serves to unify seemingly conflicting data in the literature regarding the donor properties of Ind vs Cp based on electrochemical data. It is worth noting, however, that the complexes for which the potentials of the metal-centered reduction have been measured (Table 2 and the titanocenes characterized herein) are first-row transition metal complexes, and it is unclear whether this analysis would apply with equal force to second- and third-row transition metals.

■ EXPERIMENTAL SECTION

Materials and Methods. THF, Et_2O, and CH_2Cl_2 were dried and degassed using an Innovative Technology Inc. solvent purification system. All other materials were reagent grade and used as received. Ind_2TiCl_2 was obtained from Aldrich. Reactions were performed under a dry Ar atmosphere implementing standard Schlenk procedures unless otherwise noted. $Cp_2Ti(C_2Fc)_2$[15] and $[n\text{-}Bu_4N]\text{-}[B(C_6F_5)_4]$[39] were synthesized according to literature procedures. UV−vis absorption spectra were recorded using a Cary-50 spectrophotometer. NMR spectra were obtained using a Varian 400-MR or an INOVA 500 spectrometer. Infrared spectra were measured on solid samples using a PerkinElmer Spectrum 100 series FT-IR spectrometer equipped with an ATR accessory. Cyclic voltammograms were recorded using a Pine Wavenow potentiostat controlled by Aftermath software (Pine Research Instruments). DPVs were obtained using a BASi Epsilon electrochemical workstation and a BASi cell stand. For all electrochemical experiments, the $FcH^{+/0}$ potential was measured before and/or after each experiment and all reported potentials are referenced vs this standard. Elemental analyses were performed by Midwest Microlabs in Indianapolis, IN.

Syntheses. *$Ind_2Ti(C_2Fc)_2$.* An argon-purged oven-dried two-neck round-bottom flask (25 mL) was charged with ethynlferrocene (199 mg, 0.945 mmol) and Et_2O (8 mL). After the flask was cooled in a dry ice/acetone bath for 10 min, n-butyllithium (2.5 M, 380 μL, 0.945 mmol) was added. The flask was removed from the dry ice/acetone bath and the solution stirred for 10 min. Ind_2TiCl_2 (150 mg, 0.430 mmol) was added and the solution was stirred at room temperature for 4 h. The dark green precipitate was collected using vacuum filtration. The solid was then loaded onto a silica gel column (1 cm × 12 cm) and eluted using a 5% mixture of triethylamine in CH_2Cl_2. The dark green band was collected and the solvent removed using rotary evaporation. The solid was dissolved in minimal CH_2Cl_2 (2 mL) and precipitated with hexanes (20 mL). The solid was collected using vacuum filtration, washed with Et_2O (1 mL), and dried under vacuum, yielding 126 mg (42.1%) of a dark green solid. UV−vis (THF) $\lambda_{max}(\varepsilon)$; 404 (8590), 596 (6330). UV−vis (CH_2Cl_2) $\lambda_{max}(\varepsilon)$; 407 (9210), 603 (6790). ^{1}H NMR (500 MHz, C_6D_6) δ 4.00 (dd, $J_1 = J_2 = 1.84$ Hz, 4H), 4.20 (s, 10H), 4.40 (dd, $J_1 = J_2 = 1.84$ Hz, 4H), 6.17 (d, $J = 3.09$ Hz, 4H), 6.20 (t, $J = 3.09$, Hz, 2H), 7.00 (dd, $J_1 = 3.0$ Hz, $J_2 = 6.6$ Hz, 4H), 7.51 (dd, $J_1 = 3.0$ Hz, $J_2 = 6.6$ Hz, 4H). ^{13}C NMR (400 MHz, C_6D_6) δ 159.9, 126.8, 125.9, 125.4, 119.5, 118.9, 106.4, 71.9, 70.3, 69.1, 68.1. Anal. Calcd (found) for $C_{42}H_{32}Fe_2Ti\cdot H_2O$: C, 70.62 (70.64); H, 4.80 (5.23). IR (neat) $\nu_{C\equiv C}$ = 2048 cm^{-1}.

$Ind_2Ti(C_2Fc)_2CuBr$. To an argon-purged oven-dried two-neck round-bottom flask (25 mL), dry THF (10 mL), $Ind_2Ti(C_2Fc)_2$ (100 mg, 0.144 mmol), and CuBr (41 mg, 0.287 mmol) were added. The flask was stirred at room temperature for 2 h. The solvent was removed using rotary evaporation. The solid was then loaded onto a silica gel column (1 cm × 12 cm) and eluted using a 5% mixture of triethylamine in CH_2Cl_2. The dark green band was collected and the solvent removed using rotary evaporation. The solid was dissolved in minimal CH_2Cl_2 (2 mL) and precipitated with hexanes (20 mL). The solid was collected using vacuum filtration, washed with Et_2O (1 mL), and dried under vacuum, yielding 82 mg (68%) of a dark green solid. UV−vis (THF) $\lambda_{max}(\varepsilon)$; 398 (8990), 619 (3990). UV−vis (CH_2Cl_2) $\lambda_{max}(\varepsilon)$; 392 (10000), 621 (6180). ^{1}H NMR (400 MHz, $CDCl_3$) δ 4.27 (s, 10H), 4.32 (dd, $J_1 = J_2 = 1.87$ Hz, 4H), 4.64 (dd, $J_1 = J_2 = 1.87$ Hz, 4H), 5.90 (t, $J = 3.30$ Hz, 2H), 6.00 (d, $J = 3.30$ Hz, 4H), 7.29 (dd, $J_1 = 3.1$ Hz, $J_2 = 6.5$ Hz, 4H), 7.52 (dd, $J_1 = 3.1$ Hz, $J_2 = 6.5$ Hz, 4H). ^{13}C NMR (400 MHz, $CDCl_3$) δ 145.5, 131.6, 126.8, 125.9, 123.9, 114.4, 103.3, 72.8, 70.3, 69.9, 66.1. Anal. Calcd (found) for $C_{42}H_{32}Fe_2TiCuBr$: C, 60.07 (59.77); H, 3.84 (3.99). IR (neat) $\nu_{C\equiv C}$ = 1986 cm^{-1}.

X-ray Crystallography and Crystal Structure Determination. Single crystals of $Ind_2Ti(C_2Fc)_2CuBr$ were grown in an NMR tube by layering about 5 mm of acetone and then several centimeters of hexanes onto a THF solution of the compound containing a few drops of triethylamine for long-term stability. Single crystal X-ray diffraction data were collected at 173 K using a Bruker D8 Venture diffractometer with Mo Kα radiation from an Incoatec IμS source and a Photon 100 detector. Space group determination (XPREP), structure solution (SHELXT), and structure refinement by full-matrix least-squares techniques on F2 (SHELXL) were performed using the SHELXTL software package.[40] All non-hydrogen atoms were refined anisotropically. Hydrogen atoms attached to carbon atoms were placed in geometrically optimized positions using appropriate riding models. The proper absolute structure in the non-centrosymmetric space group $Fdd2$ is supported by the Flack parameter of 0.051(5). Further details of the refinement and crystallographic data are given in the Supporting Information and are available through the Cambridge Crystallographic Data Centre, CCDC deposition number 1968308.

■ ASSOCIATED CONTENT

Ⓢ Supporting Information

The Supporting Information is available free of charge at https://pubs.acs.org/doi/10.1021/acs.organomet.9b00818.

^{1}H and ^{13}C NMR spectra for $Ind_2Ti(C_2Fc)_2$ and $Ind_2Ti(C_2Fc)_2CuBr$, crystallographic data for $Ind_2Ti(C_2Fc)_2CuBr$ and several different orientations and packing arrangement for it structure, UV−vis spectra in THF, sweep-rate dependence of the cathodic wave for $Ind_2Ti(C_2Fc)_2$, effect of reversal potential on the anodic waves for $Ind_2Ti(C_2Fc)_2$ (PDF)

Structure data (XYZ)

Accession Codes

CCDC 1968308 contains the supplementary crystallographic data for this paper. These data can be obtained free of charge via www.ccdc.cam.ac.uk/data_request/cif, or by emailing data_request@ccdc.cam.ac.uk, or by contacting The Cambridge Crystallographic Data Centre, 12 Union Road, Cambridge CB2 1EZ, UK; fax: +44 1223 336033.

■ AUTHOR INFORMATION

Corresponding Author

Paul S. Wagenknecht − *Department of Chemistry, Furman University, Greenville, South Carolina 29609, United States;* ● orcid.org/0000-0001-8698-073X; Email: paul.wagenknecht@furman.edu

Authors

Khiem T. Nguyen − *Department of Chemistry, Furman University, Greenville, South Carolina 29609, United States*

Emily E. Lane − *Department of Chemistry, Furman University, Greenville, South Carolina 29609, United States*

Colin D. McMillen − *Department of Chemistry, Clemson University, Clemson, South Carolina 29634, United States;* orcid.org/0000-0002-7773-8797

Jared A. Pienkos − *Department of Chemistry, Furman University, Greenville, South Carolina 29609, United States*

Complete contact information is available at:
https://pubs.acs.org/10.1021/acs.organomet.9b00818

Notes

The authors declare no competing financial interest.

■ REFERENCES

(1) Kealy, T. J.; Pauson, P. L. A new type of organo-iron compound. *Nature* **1951**, *168*, 1039−1040.

(2) (a) Wilkinson, G.; Rosenblum, M.; Whiting, M. C.; Woodward, R. B. The structure of iron *bis*-cyclopentadienyl. *J. Am. Chem. Soc.* **1952**, *74*, 2125−2126. (b) Fischer, E. O.; Pfab, W. On the crystal structure of the bis-cyclopentadienyl compounds of divalent iron, cobalt and nickel. *Z. Anorg. Allg. Chem.* **1952**, *7*, 377−379.

(3) Trost, B. M.; Ryan, M. C. Indenylmetal catalysis in organic synthesis. *Angew. Chem., Int. Ed.* **2017**, *56*, 2862−2879.

(4) Hart-Davis, A. J.; Mawby, R. J. Reactions of R-lndenyl Complexes of Transition Metals. Part 1. Kinetics and Mechanisms of Reactions of Tricarbonyl-π–indenylmethylmolybdenum with Phosphorus(III) Ligands. *J. Chem. Soc. A* **1969**, *0*, 2403−2407.

(5) (a) Rerek, M. E.; Ji, L.-N.; Basolo, F. The Indenyl Ligand Effect on the Rate of Substitution Reactions of $Rh(\eta-C_9H_7)(CO)_2$ and $Mn((\eta-C_9H_7)(CO)_3$. *J. Chem. Soc., Chem. Commun.* **1983**, 1208−1209. (b) O'Connor, J. M.; Casey, C. P. Ring-slippage chemistry of transition metal cyclopentadienyl and indenyl complexes. *Chem. Rev.* **1987**, *87* (2), 307−318.

(6) Cadierno, V.; Díez, J.; Gamasa, M. P.; Gimeno, J.; Lastra, E. Indenyl complexes of Group 8 metals. *Coord. Chem. Rev.* **1999**, *193−195*, 147−205.

(7) Calhorda, M. J.; Romão, C. C.; Veiros, L. F. The Nature of the Indenyl Effect. *Chem. - Eur. J.* **2002**, *8* (4), 868−875.

(8) Crossley, N. S.; Green, J. C.; Nagy, A.; Stringer, G. Electronic structure of transition-metal indenyl compounds: a He I and He II photoelectron spectroscopic study of $[Mn(\eta^5-C_9H_7)(CO)_3]$, $[Fe(\eta^5-C_9H_7)_2]$, $[Ru(\eta^5-C_9H_7)_2]$, and $[Ru(\eta^5-C_9H_7)\eta-C_5Me_5)]$. *J. Chem. Soc., Dalton Trans.* **1989**, No. 11, 2139−2147.

(9) Frankcom, T. M.; Green, J. C.; Nagy, A.; Kakkar, A. K.; Marder, T. B. Electronic structure and photoelectron spectroscopy of d^8 rhodium indenyl complexes. *Organometallics* **1993**, *12* (9), 3688−3697.

(10) Ambrosi, L.; Bassetti, M.; Buttiglieri, P.; Mannina, L.; Monti, D.; Bocelli, G. Synthesis and structure of acylcarbonylindenyl-(phosphine) iron(II). *J. Organomet. Chem.* **1993**, *455* (1−2), 167−175.

(11) Gamasa, M. P.; Gimeno, J.; González-Bernardo, C.; Martín-Vaca, B. M.; Monti, D.; Bassetti, M. Phosphine Substitution in Indenyl- and Cyclopentadienylruthenium Complexes. Effect of the η^5 Ligand in a Dissociative Pathway. *Organometallics* **1996**, *15* (1), 302−308.

(12) Pauson, P. L.; Wilkinson, G. Bis-indenyl Derivatives of Iron and Cobalt. *J. Am. Chem. Soc.* **1954**, *76* (7), 2024−2026.

(13) Samuel, E.; Hénique, J. Phosphine complexes of Ti(III) and Zr(III): detection in solution by EPR/electrochemical methods. *J. Organomet. Chem.* **1996**, *512* (1−2), 183−187.

(14) Miller, G. A.; Therien, M. J.; Trogler, W. C. Electrochemical studies of an oxidatively induced ring slippage in 17-electron (η^3-indenyl)(η^5-indenyl)V(CO)$_2$. *J. Organomet. Chem.* **1990**, *383* (1−3), 271−278.

(15) Turlington, M. D.; Pienkos, J. A.; Carlton, E. S.; Wroblewski, K. N.; Myers, A. R.; Trindle, C. O.; Altun, Z.; Rack, J. J.; Wagenknecht, P. S. Complexes with Tunable Intramolecular Ferrocene to Ti^{IV} Electronic Transitions: Models for Solid State Fe^{II} to Ti^{IV} Charge Transfer. *Inorg. Chem.* **2016**, *55*, 2200−2211.

(16) Pienkos, J. A.; Webster, A. B.; Piechota, E. J.; Agakidou, A. D.; McMillen, C. D.; Pritchett, D. Y.; Meyer, G. J.; Wagenknecht, P. S. Oxidatively stable ferrocenyl-π-bridge-titanocene D-π-A complexes: an electrochemical and spectroscopic investigation of the mixed-valent states. *Dalton Trans.* **2018**, *47*, 10953−10964.

(17) Livshits, M. Y.; Turlington, M. D.; Trindle, C. O.; Wang, L.; Altun, Z.; Wagenknecht, P. S.; Rack, J. J. Picosecond to Nanosecond Manipulation of Excited-State Lifetimes in Complexes with an Fe^{II} to Ti^{IV} Metal-to-Metal ChargeTransfer: The Role of Ferrocene-Centered Excited States. *Inorg. Chem.* **2019**, *58*, 15320−15329.

(18) Back, S.; Rheinwald, G.; Lang, H. Synthesis, electrochemistry and electronic spectra of tetranuclear bis(η^2-alkynyl) transition-metal complexes. The molecular structure of $[(\eta^5-C_5H_4SiMe_3)_2Ti-(CCFc)]_2CuBr$. *J. Organomet. Chem.* **2000**, *601*, 93−99.

(19) Back, S.; Stein, T.; Frosch, W.; Wu, I.-Y.; Kralik, J.; Büchner, M.; Huttner, G.; Rheinwald, G.; Lang, H. Heterometallic early-late H-tweezer complexes: their synthesis, electrochemical behaviour, and the solid state structures of $(\eta^5-C_5H_4SiMe_3)_2Ti(CCPh)_2$ and $[(\eta^5-C_5H_4SiMe_3)_2Ti(CCPh)_2]Pd(PPh_3)$. *Inorg. Chim. Acta* **2001**, *325*, 94−102.

(20) Vieira, N. C.; Pienkos, J. A.; McMillen, C. D.; Myers, A. R.; Clay, A. P.; Wagenknecht, P. S. A *trans*-bidentate bis-pyridinyl ligand with a transition metal hinge. *Dalton Trans.* **2017**, *46*, 15195−15199.

(21) Faller, J. W.; Crabtree, R. H.; Habib, A. Control of Slippage and Conformation in Indenyl Complexes. *Organometallics* **1985**, *4*, 929−935.

(22) Westcott, S. A.; Kakkar, A. K.; Stringer, G.; Taylor, N. J.; Marder, T. B. Flexible coordination of indenyl ligands in sandwich complexes of transition metals. Molecular structures of $[(\eta-C_9R_7)_2M]$ (M = Fe, R = H, Me; M = Co, Ni, R = H): Direct measurement of the degree of slip-fold distortion as a function of d-electron count. *J. Organomet. Chem.* **1990**, *394*, 777−794.

(23) Back, S.; Pritzkow, H.; Lang, H. C$_2$-Bridged Titanocene-Ferrocenyl Complexes: Synthesis, Reaction Chemistry, and Electrochemical Behavior. *Organometallics* **1998**, *17*, 41−44.

(24) Hayashi, Y.; Osawa, M.; Wakatsuki, Y. Reductive coupling reaction induced by remote-site oxidation in titaocene bis-(metallocenylacetylide), where metallocenyl = ferrocenyl or ruthenocenyl: a novel route to C$_n$ (n = 4, 6, and 8) wire with the metallocenyl groups at both terminals. *J. Organomet. Chem.* **1997**, *542*, 241−246.

(25) Barrière, F.; Camire, N.; Geiger, W. E.; Mueller-Westerhoff, U. T.; Sanders, R. Use of Medium Effects to Tune the UE$_{1/2}$ Values of Bimetallic and Oligometallic Compounds. *J. Am. Chem. Soc.* **2002**, *124*, 7262−7263.

(26) Diallo, A. K.; Absalon, C.; Ruiz, J.; Astruc, D. Ferrocenyl-Terminated Redox Stars: Synthesis and Electrostatic Effects in Mixed-Valence Stabilization. *J. Am. Chem. Soc.* **2011**, *133*, 629−641.

(27) Treichel, P. M.; Johnson, J. W.; Wagner, K. P. Electrochemical oxidations of various indenyl—iron complexes. *J. Organomet. Chem.* **1975**, *88* (2), 227−230.

(28) Hill, M. G.; Lamanna, W. M.; Mann, K. R. Tetrabutylammonium tetrakis[3,5-bis(trifluoromethyl)phenyl]borate as a noncoordinating electrolyte: Reversible 1e- oxidations of ruthenocene, osmocene, and Rh$_2$(TM4)$_4^{2+}$ (TM4 = 2,5-diisocyano-2,5-dimethylhexane). *Inorg. Chem.* **1991**, *30*, 4687−4690.

(29) Kukharenko, S. V.; Strelets, V. V.; Kudinov, A. R.; Kreidlin, A. Z.; Peterleitner, M. G.; Denisovich, L. I.; Rybinskaya, M. I. Reactivity of 17- and 19-electron organometallic complexes. Formation of bent sandwich 19-electron radical cation complexes of osmium and ruthenium. *J. Organomet. Chem.* **1996**, *519* (1−2), 1−5.

(30) Geiger, W. E. Electroreduction of Cobaltocene. Evidence for a Metallocene Anion. *J. Am. Chem. Soc.* **1974**, *96*, 2632−2634.

(31) Knizhnikov, V. A.; Shirokii, V. L.; Dikusar, E. A.; Ryabtsev, A. N.; Maier, N. A. Derivatives of bis(η^5-indenyl)cobalt. *Russ. J. Gen. Chem.* **1997**, *67* (10), 1634−1637.

(32) Weiß, T.; Natarajan, K.; Lang, H.; Holze, R. Indenyl-titaniumtrichloride complexes: correlations between electrochemical and UV-vis-spectroscopic data. *J. Electroanal. Chem.* **2002**, *533* (1−2), 127−133.

(33) Kowaleski, R. M.; Rheingold, A. L.; Trogler, W. C.; Basolo, F. Synthesis and Structure of Dicarbonyl(η^3-indenyl)(η^5-indenyl)-vanadium(II). An Unusual Slipped Ring in a Metal Radical. *J. Am. Chem. Soc.* **1986**, *108*, 2460−2461.

(34) Gamelas, C. A.; Herdtweck, E.; Lopes, J.; Romao, C. C. Redox-Induced Indenyl Slippage in [IndCpMoL$_2$]$^{2+/+/0}$ Complexes. *Organometallics* **1999**, *18*, 506−515.

(35) Lee, S.; Lovelace, S. R.; Cooper, N. J. Two-Electron and One-Electron Reduction of the Indenyl Complex [Mn(η^5-C$_9$H$_7$)(CO)$_3$] and Reversible Counterion-Controlled Comproportionation of [Mn(η^5-C$_9$H$_7$)(CO)$_3$] and [Mn(η^3-C$_9$H$_7$)(CO)$_3$]$^{2-}$ To Give [Mn(η^5-C$_9$H$_7$)(CO)$_3$]$^-$. *Organometallics* **1995**, *14*, 1974−1982.

(36) (a) Allen, G. C.; Hush, N. S. Intervalence-Transfer Absorption. Part 1. Qualitative Evidence for Intervalence-Transfer Absorption in Inorganic Systems in Solution and in the Solid State. *Prog. Inorg. Chem.* **2007**, *8*, 357−444. (b) Creutz, C. Mixed Valence Complexes of d^5-d^6 Metal Centers. *Prog. Inorg. Chem.* **1983**, *30*, 1−73. (c) Katz, N. E.; Creutz, C.; Sutin, N. 4-Cyanopyridine-bridged binuclear and trinuclear complexes of ruthenium and iron. *Inorg. Chem.* **1988**, *27*, 1687−1694. (d) Bernhardt, P. V.; Macpherson, B. P.; Martinez, M. The influence of *cis/trans* isomerism on the physical properties of a cyano-bridged dinuclear mixed valence complex. *J. Chem. Soc., Dalton Trans.* **2002**, 1435−1441.

(37) Ratera, I.; Sporer, C.; Ruiz-Molina, D.; Ventosa, N.; Baggerman, J.; Brouwer, A. M.; Rovira, C.; Veciana, J. Solvent Tuning from Normal to Inverted Marcus Region of Intramolecular Electron Transfer in Ferrocene-Based Organic Radicals. *J. Am. Chem. Soc.* **2007**, *129*, 6117−6129.

(38) Brunschwig, B. S.; Ehrenson, S.; Sutin, N. Solvent Reorganization in Optical and Thermal Electron-Transfer Processes. *J. Phys. Chem.* **1986**, *90*, 3657−3668.

(39) LeSuer, R. J.; Buttolph, C.; Geiger, W. E. Comparison of the Conductivity Properties of the Tetrabutylammonium Salt of Tetrakis(pentafluorophenyl)borate Anion with Those of Traditional Supporting Electrolyte Anions in Nonaqueous Solvents. *Anal. Chem.* **2004**, *76*, 6395−6401.

(40) Sheldrick, G. M. Crystal Structure Refinement with SHELXL. *Acta Crystallogr., Sect. C: Struct. Chem.* **2015**, *71*, 3−8.